SLAC–PUB–12337
February 2007

High-Efficiency Absorber for Damping Transverse Wake Fields *

A. Novokhatski, J. Seeman, S. Weathersby
Stanford Linear Accelerator Center, 2575 Sand Hill Road, Menlo Park, California 94025

Abstract

Transverse wake fields generated by intense beams may propagate long distances in the vacuum chamber and dissipate power in different shielded elements such as bellows, vacuum valves or vacuum pumps. Induced heating in these elements may be high enough to deteriorate vacuum conditions. We have developed a broadband water-cooled bellows-absorber to capture and damp these harmful transverse fields without impacting the longitudinal beam impedance. Experimental results at the PEP-II SLAC B-factory demonstrate high efficiency of this device. This absorber may be useful in other machines like synchrotron light sources or International Linear Collider.

Submitted to

Physical Review Special Topics - Accelerators and Beams (PRST-AB)

* Work supported by Department of Energy contract DE–AC02–76SF00515.

High-Efficiency Absorber for Damping Transverse Wake Fields

A. Novokhatski,* J. Seeman, and S. Weathersby
SLAC, Stanford University, 2575 Sand Hill Road, Menlo Park, CA 94025, USA
(Dated: February 21, 2007)

Transverse wake fields generated by intense beams may propagate long distances in the vacuum chamber and dissipate power in different shielded elements such as bellows, vacuum valves or vacuum pumps. Induced heating in these elements may be high enough to deteriorate vacuum conditions. We have developed a broadband water-cooled bellows-absorber to capture and damp these harmful transverse fields without impacting the longitudinal beam impedance. Experimental results at the PEP-II SLAC B-factory demonstrate high efficiency of this device. This absorber may be useful in other machines like synchrotron light sources or International Linear Collider.

PACS numbers: 29.20.-c; 42.25.Dd; 84.40.-x

I. INTRODUCTION

The SLAC PEP-II asymmetric B-factory collides 1700 bunches of 3.0 A of 3 GeV positrons on 1.9 A of 9 GeV electrons. B-factory consists of a low energy positron storage ring (LER) situated above a high energy electron storage ring (HER). The rings intersect at an interaction point (IP) within the BaBar detector sustaining a luminosity of $1.2 \times 10^{34} cm^{-2}s^{-1}$ [1]. Very low longitudinal impedance of the vacuum chamber allowed us to achieve extremely high currents.

However we found elevated temperature on shielded bellows and vacuum valves around the rings. Longitudinal wake fields have very small coupling with shielded bellows cavities, but transverse fields can easily penetrate through the fingers and excite different resonant modes. As transverse fields may propagate long distances in aluminum chamber the wake field source can be far away from the bellows position. Of particular concern were anomalously high temperatures observed on a first arc bellows, located 15 meters downstream of a fixed vertical beam collimator. Thermocouples mounted on the exterior of the bellows within the convolutions were registering a temperature rise of 80°F reaching 220°F at nominal LER currents of 2500 mA even after the installation of cooling fans. Internally, sensitive bellows fingers can reach much higher temperatures. In this region the power in the wake fields was high enough to destroy the feed-through for the titanium sublimation pump. In order to solve this problem we installed an arc absorber directly in the ante-chamber part of the pumping section to capture these wake fields [2]. The power loss in the absorber reaches 1200 W for a positron beam current of 2.4 A. This arc absorber helped to find the source of wake fields. Steering the beam at the vertical collimator upstream of the absorber resulted in the significant power change in the absorber. There was no power change when we tried to steer the beam at the horizontal collimator. So only fields with vertical polarization propagate in this pumping chamber. However the temperature rise in the upstream arc bellows correlates with beam steering at both collimators [3].

The requirement for higher luminosity entails higher ring currents at the 3-4 A levels as well as shorter bunch lengths of 0.8 cm, both of which will contribute to more bellows heating. To solve this problem we have used our understanding of the wake field nature to design a special absorber.

In the absorbers, which were developed to damp Higher Order Modes (HOM) near RF cavities the absorbing material is usually exposed to the beam. This causes additional beam energy losses due to diffraction of the beam field and Cherenkov radiation, when absorbing material has noticeable permittivity or magnetic permeability [4],[5], [6]. The design of a wing-type HOM damper [7] needs too much space in the ring. There are two slots with length of 600 mm. It was designed to damp only one polarization of the dipole like modes and consequently has less efficiency for quadrupole-like modes. In our case we had only 70 mm space for slots. We optimized the geometry of absorbing tiles, the number of slots and their width to avoid additional losses from the longitudinal fields while efficiently damping all transverse fields. The proposal for absorber was presented at PAC'2005 [3],[8] and first results were presented at EPAC'2006 [9].

II. COLLIMATOR WAKE FIELDS

In addition to measurement in the ring we carry out numerical studies of wake fields excited near a collimator using MAFIA code [10]. The shape of the PEP-II LER straight section collimator is shown in Figure 1. It consists of a central flat protrusion inside a round chamber. The protrusion has tapers at both ends. The total length is 60.8 cm. We did simulations for the vertical collimator, which has 9 mm nominal offset from the collimator edge to the beam axis. We compute the loss factor of a 13 mm long Gaussian bunch passing the vertical collimator at different off-sets in vertical and horizontal positions relative to the collimator. Results, which are shown in Figure 2 confirm measurements. When we move the beam

*Electronic address: novo@slac.stanford.edu

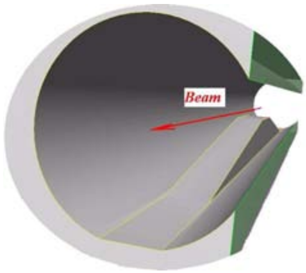

FIG. 1: PEP-II LER collimator.

closer to the collimator edge in the vertical direction the arc absorber sees more power. When we move the beam in the horizontal direction the power in absorber did not change much.

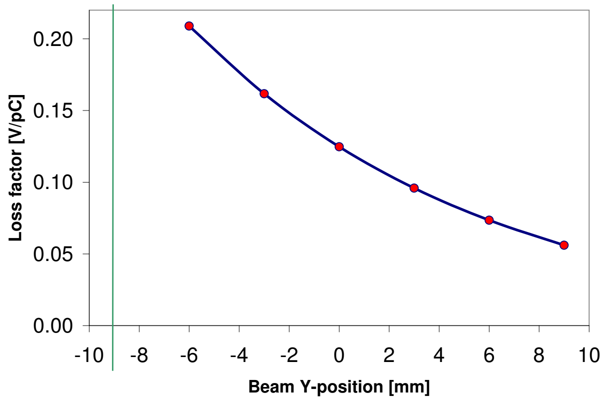

FIG. 2: Loss factor of a 13 mm long Gaussian bunch passing the vertical collimator at different off-sets in the vertical positions. Green line shows collimator edge.

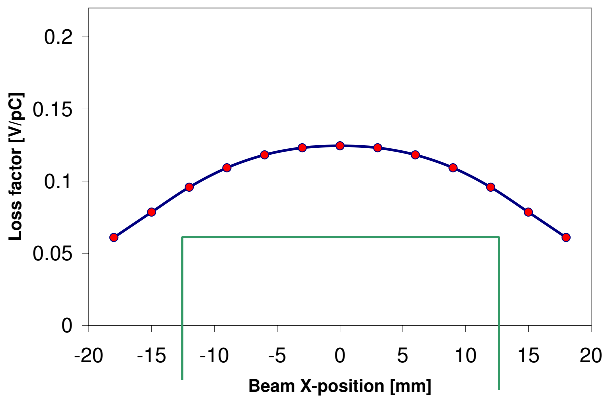

FIG. 3: Loss factor of a 13 mm long Gaussian bunch passing the vertical collimator at different off-sets in the horizontal position. Green line shows collimator edge.

Loss factor k beam current I and bunch spacing τ gives the power generated by the beam

$$P = k \times \tau \times I^2 \tag{1}$$

For the current beam parameters: I=2.4 A, τ=4.2 nsec

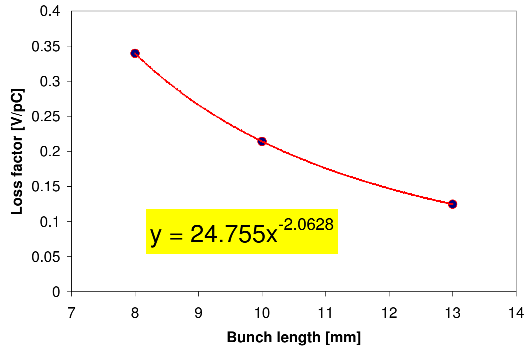

FIG. 4: Loss factor as a function of bunch length.

(bunch spacing by 2) and k=0.125V/pC (bunch length σ=13 mm at nominal position of the beam near the collimator) this power is 3 kW. This number looks to be reasonable. We measured captured power in the arc absorber of 1.2 kW. The arc absorber is 15 m far away from collimator, so some power is dissipated in the chamber wall. Some power goes to the bellows, a vacuum valve or propagates to the next arc chambers. (We will get better estimation of collimator wake field power with a new bellows absorber). Calculated bunch length dependence of the loss factor (Figure 4) is well approximated with an inverse quadratic function. This is also in agreement with measurement of the power in arc absorber, which is linear with RF voltage [2] and is equivalent to the inverse quadratic dependence on the bunch length.

In simulations we found the direction of the wake field energy flow to be the same as in experiment. Steering the beam at the collimator we found the temperature change only in the bellows, which are downstream to collimator. Figure 5 shows the calculated energy flow at two end of the collimator. Energy flow was calculated as the integral of the Poynting vector over the chamber cross section

$$\frac{d\epsilon}{dt} = \oint (\vec{E} \times \vec{H}) \cdot d\vec{s} \tag{2}$$

In Figure 5 a positive energy flow indicates flow in the beam direction. Negative flow is in the upstream direction. The double peak shape of upstream energy flow originates at the two sloped faces of the collimator.

Calculated frequency spectrum of the collimator wake field of a 13 mm long Gaussian bunch was also found to be similar to the spectrum measurement. A spectrum analyzer and antenna were installed in the tunnel near the TSP feed-through [2]. Figure 6 shows the measured spectrum in a multi bunch regime. Figure 7 shows calculated wake field spectrum of a single bunch. Spectrum has maximum in the frequency range of 2-3 GHz (cut-off frequency for TE_{11} mode is 1.99 GHz). It is important to note that there is a set of high Q trapped collimator modes [11, 12], which give additional heating to the collimator. Naturally these modes stay near collimator and do not propagate in the ring.

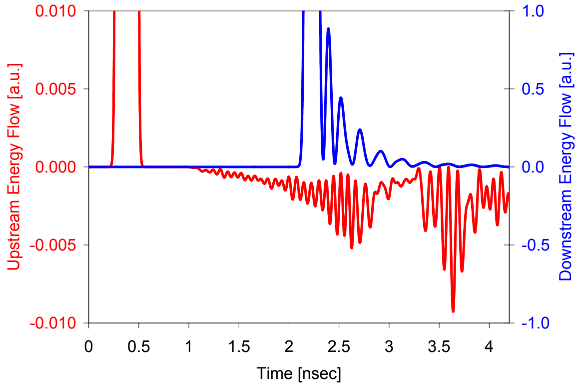

FIG. 5: Time dependence of the energy flow through the incoming (red) and outcoming (blue) chamber cross sections of the collimator. Scales are 100 times different.

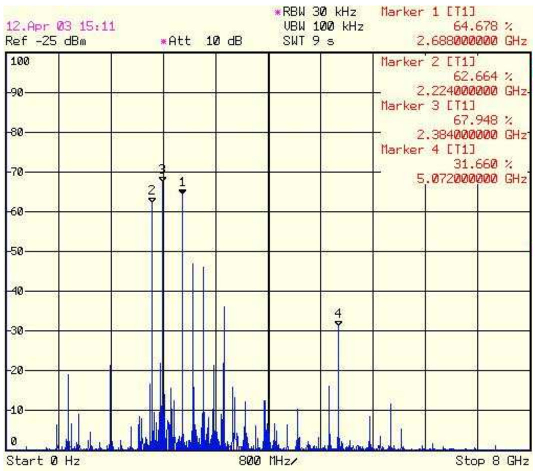

FIG. 6: Wake field spectrum measured in the PEP-II tunnel in a multi bunch regime.

We also study the detailed structure of the wake fields. It was determined that collimator wake fields have mainly the form of dipole and quadrupole propagating modes. Figure 8 shows snapshots of electric field force lines downstream from the collimator during one nanosecond after the passage of a bunch. They have a dipole and quadrupole field pattern. The dipole mode predominates. Based on these studies a device was designed to specifically couple out and damp dipole, quadrupole and higher modes while leaving the longitudinal (monopole) mode untouched. The coupled mode power is concentrated and dissipated in water cooled ceramic tiles.

III. STRAIGHT SECTION BELLOWS-ABSORBER

We consider a device with coupling slots and a cavity containing high loss tangent ceramic tiles. We combine a shielded bellows and an absorber in one device: bellows-

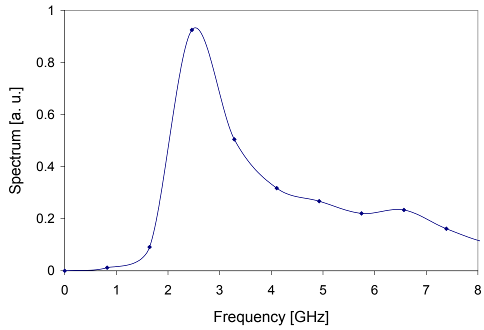

FIG. 7: Calculated spectrum of the collimator wake field of a single bunch.

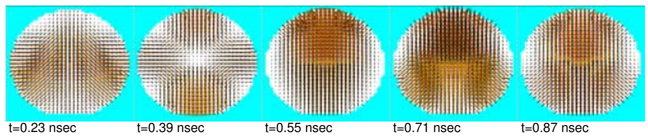

FIG. 8: Electric field force lines downstream from the collimator at consecutive time periods after the passage of a bunch.

absorber.

A. Ceramic tiles characterization

SLAC has extensive experience [13] in using Ceradyne inc. [14] ceramic tiles as effective absorbing material. We successfully used these tiles in the arc absorber [2]. The material of a tile (Ceralloy 13740Y) consists of AlN with 40% SiC. Although the company gives the table of dielectric properties of this material we measured the relative permittivity and loss tangent at S-band frequency. We used the fact that the resonant frequency f_d of a cavity depends upon relative permittivity ϵ of the material that filling a cavity

$$f_d = f_0/\sqrt{\epsilon} \tag{3}$$

where f_0 is resonant frequency of an empty cavity. Additionally for high loss materials the inverse value of the resonance quality factor Q_d is almost equal to loss tangent $\tan\delta$

$$\frac{1}{Q_d} =\approx \tan\delta \tag{4}$$

when the Q-value of the empty cavity is high. For the measurement we used a copper rectangular box, which has the same inner sizes as a ceramic tile. The empty copper cavity has Q-value of several thousand. The photo of this box and the tile is shown in Figure 9. Ceramic tile dimensions are $14.22mm \times 14.58mm \times 5.94mm$. The lowest resonant frequency of the empty cavity is 14.72 GHz. When we place a tile inside the cavity the resonant frequency drops to 3.27 GHz, equivalent to a relative permittivity 20.3. Q-measurement resulted in loss tangent

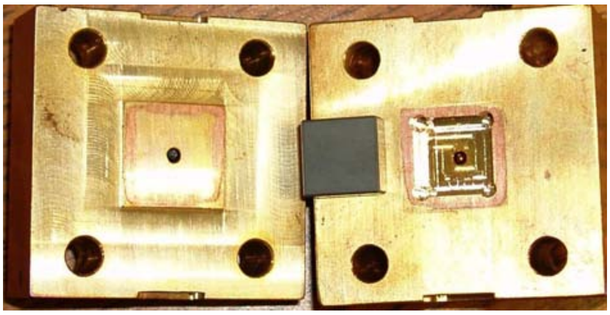

FIG. 9: Copper cavity with two antennas to measurer the dielectric constant and loss tangent of a ceramic tile.

$\tan\delta = 0.25$. Ceradyne's table [14] gives dielectric parameters only for three frequencies: 1, 8 and 10 GHz. Based on these numbers we approximated its parameters at 3.3 GHz: relative permittivity 26.6 and loss tangent 0.22. We measured several tiles and found that their parameters do not differ much. Relative permittivity deviates within $\pm 3.5\%$ and loss tangent $\pm 2.2\%$. However we found strong temperature dependance. Results of temperature measurement are shown in Figure 10. Loss tangent drops to almost 0.1 and relative permittivity rises up to 25 when temperature reaches 250° F. Assuming that

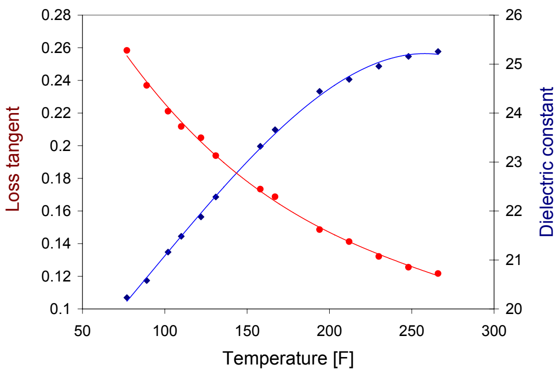

FIG. 10: Temperature dependence of the dielectric constant(blue) and loss tangent (red) from our measurement.

working temperature of tiles could be high we choose the following parameters $\epsilon = 30$, $\tan\delta = 0.1$ to be used in computer modeling of the straight absorber.

B. Coupling slots

We want to damp transverse fields, which have transverse electric component and longitudinal magnetic component. On contrary we want to keep the bunch field, which has transverse magnetic and electric component. To couple out only transverse fields and not bunch field we will use thin longitudinal slots. This slots couple out fields with magnetic field parallel to slots and couple much less the fields with magnetic field transverse to slots. If a slot has an elliptical shape with semi major axis l and semi-minor axis d and ellipse is narrow $l \gg d$, then the coupling of transverse field according to [15] is

$$k_\perp \propto \frac{\pi}{3} \frac{l^3}{\ln \frac{4l}{d} - 1} \tag{5}$$

coupling of the bunch field is

$$k_b \propto \frac{\pi}{3} l d^2 \tag{6}$$

The ratio between couplings k_b to $k_\perp$ depends upon the ratio of axes $(d/l)^2$ and can be made very small. On the other hand the coupling of transverse modes is proportional to the cube of the slot length and can be large enough to transfer out almost all the mode power. For this we will need a slot length of order of the tube diameter.

C. Computer modeling of the bellows-absorber

In order to place an absorber in the PEP-II low energy ring we decided to replace an existing shielded bellows module by a new design. In a new design we decrease the bellows convolution length and use all free space for absorber slots. In this way we managed to find 70 mm for the absorber. The geometry of the absorber vacuum chamber assembly (one quarter) is depicted in figure 11. The vacuum chamber assembly has an annular cavity which houses the bellows assembly and a set of ceramic bricks or tiles (dark gray) separated from the beam chamber by a series of longitudinal coupling slots. This offers a conductive path for monopole like beam fields while exposing the absorbing material to the transverse fields (dipole and quadrupole). The absorbing tiles are brazed to a copper block with cooling water pipes to extract the heat. The absorber cavity features an extension which exposes the bellows cavity to the absorber. This has the added effect of damping any modes which might be produced by the transverse fields coupling into the bellows through the bellows fingers. However for computer simulations we ignore the bellows thin fingers and simplify the bellows convolutions. We use s-parameter analysis

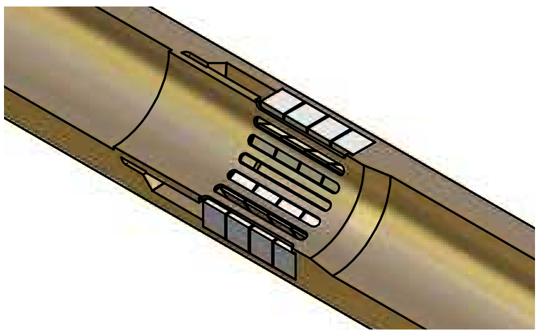

FIG. 11: The model of the bellows-absorber (one quarter).

to characterize the behavior of an absorber configuration (geometry and material parameters). This capability is included in the MAFIA package [10]. a simulated electromagnetic wave packet of a chosen frequency range propagates through the beam pipe incorporating an absorber structure. We simulate each type of transverse mode: monopole, dipole and quadrupole, which is perfectly match at the "mesh" entry and "mesh" exit of absorber structure in order to simulate the "half-infinite waveguides" before and after the configuration. The amplitudes of the fields are monitored in time at the entry and exit ports of the structure. The length of the simulated configuration is chosen to be several times longer than the wave packet length in order to separate forward and backward waves. Then the Fourier transform of the amplitudes gives transmission s_{21} and reflection s_{11} coefficients in the chosen frequency range. Fractional power loss (or absorption) is calculated from the energy conservation law: $P = 1 - s_{11}^2 - s_{21}^2$.

The computer design process involved variation of slot, absorber and cavity geometry to optimize absorption characteristics using scattering parameter analysis. We optimized the absorber configuration parameters in order to maximize absorption for dipole and quadrupole modes at the given slot length of 70 mm. At first we study how the thickness of the slots influences absorption. To limit the image current density at a double value we choose the slot thickness to be the same thickness the metal part between slots. Under this condition we determine the number of slots for different slot thickness. We found that thicker slots give more absorption, but also increase the absorption for the monopole (longitudinal) mode, which is undesirable. We choose a compromise for slot thickness of 6 mm that gives less than 1% absorption for the monopole mode. Then we optimize the thickness of tiles and determined that the frequency spectrum follows the tile thickness. Thicker tiles move the spectrum to the low frequency range. The tiles thickness of 16.7 mm give a more or less flat frequency spectrum in the range 2 to 7 GHz. Results of scattering parameter analysis for the optimized absorber configuration for three waveguide modes: monopole (top), dipole (middle) and quadrupole (bottom) are shown in Fig. 12. Average absorption of

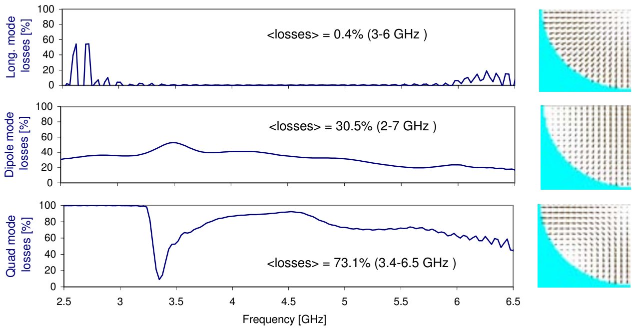

FIG. 12: Losses of different type of modes in absorber. The insets show electric force lines for each mode.

longitudinal mode is around 0.4% in the frequency range of 3 to 6 GHz. Dipole mode absorption is important since this is the main mode generated by the collimator. In the 2-7 GHz range we can expect on average 31% of the dipole mode power to be absorbed. Maximum absorption of 53% is at the frequency of 3.5 GHz over a surrounding 40% plateau. Absorption of the quadrupole mode is on average of 73% in the frequency range of 3.4-6.5 GHz. Low frequency limit is determined by cut-off frequency of each mode.

D. Bellows-absorber measurement

Based on computer modeling a bellows-absorber was designed and four absorbers were produced. Figure 13 shows the photo of completed device just prior to installation. From the photo it is possible to see shielded bellows fingers (white) and coupling absorber slots in the tube (red). Absorbing tiles (gray) are seen behind coupling slots. Copper water cooling lines remove absorber HOM power. The cooling system was designed to take out more than 10 kW HOM power. The first bellows-

FIG. 13: Bellows-absorber

absorber was installed in the Low Energy Ring (LER) in region 4 at the end of a straight and has experienced high current running. The bellows-absorber position in the ring is shown in Figure 14. Downstream we have a vacuum valve and an arc bellows. This arc bellows has intense air-cooling, it has the maximum temperature rise in the ring. Next we have a quadrupole magnet, a bending magnet and first arc pumping chamber, which has an absorber in its ante-chamber.

To determine the effect of the bellows-absorber we measure the temperature of the arc bellows (see photo 14) before and after installation of the bellows-absorber. Fig. 15 shows the history of the temperature rise in the arc bellows (red) and LER current (green). After installation of the bellows-absorber on May 1, 2006 the arc bellows temperature drops to almost half of the previous value at comparable LER currents. Pump ports, vacuum valves and anti-chambers see a similar reduction.

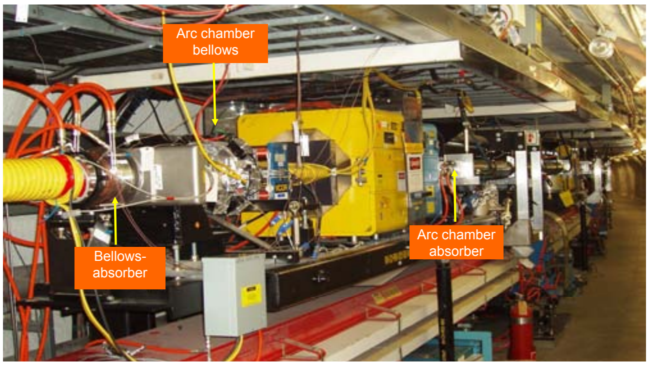

FIG. 14: SLAC PEP-II tunnel where the bellows-absorber is installed.

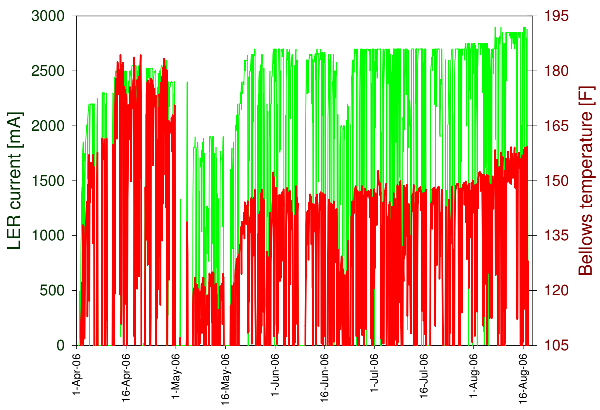

FIG. 15: Temperature rise in the downstream arc bellows (red) and LER current (green)

Efficiency of the bellows-absorber was evaluated from the HOM power measurement in the arc chamber absorber. Figure 16 shows the current dependence of the HOM power in this absorber before and after installation of the bellows-absorber. We are reminded that the arc chamber absorber takes HOM power only from the vertical collimator.

The HOM power dependence is quadratic with LER current. A fit for the coefficient with data from before and after the installation gives 145 and 82 W/mA^2 respectively. The ratio of the coefficients gives a 42% reduction in power. That means that the bellows-absorber captures 42% of the HOM power generated at the vertical collimator. Power in the absorber as a function of the beam current is shown in Figure 17 for two different RF voltages. For the LER current of 2.4 A the HOM power captured in the bellows-absorber reaches 1.45 KW. Knowing the efficiency of the absorber we can estimate the HOM power coming from the vertical collimator at this current

$$P_{v.c.} = 1.45kW/0.42 = 3.45kW \tag{7}$$

This number is very close to the result of wake field calculation presented in section II.

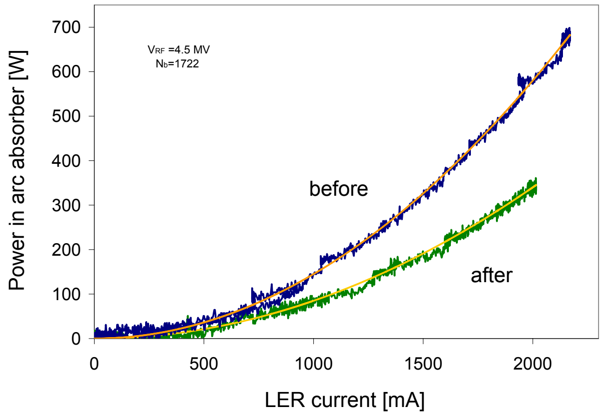

FIG. 16: HOM power in the downstream arc absorber before (dark blue) and after (green) installation of the bellows-absorber. Orange and yellow lines show quadratic fit.

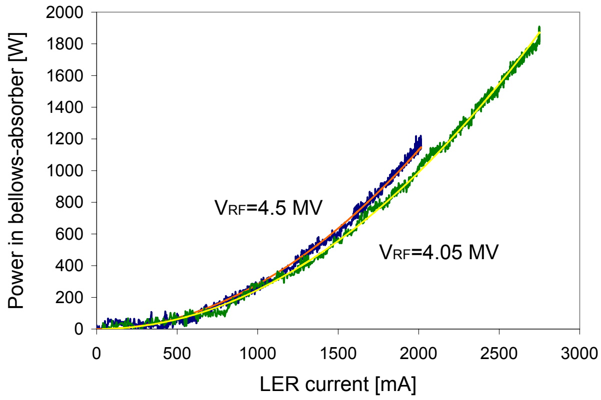

FIG. 17: Power in bellows-absorber for different RF voltages.

After successful results with the first bellows-absorber we installed two other absorbers in the same straight section of region 4 but downstream to two horizontal collimators. An additional bellows-absorber was installed in the straight section of region 10.

IV. HIGH EFFICIENCY ABSORBER FOR INTERACTION REGION

As we discussed earlier the coupling of transverse fields and respectively the efficiency of the HOM absorber strongly depends upon the length of the coupling slots. Can we design a more efficient absorber with almost full absorption by increasing the slot length? We study this possibility for absorber, which we plan to install in the Interaction Region (IR), as we have more space there. Unlike the straight section chamber in region 4 the IR vacuum chamber has an octagonal shape. Now vertical and horizontal polarization of transverse modes are different and separated in frequency. Different polarizations may have different absorption. We found that this differ-

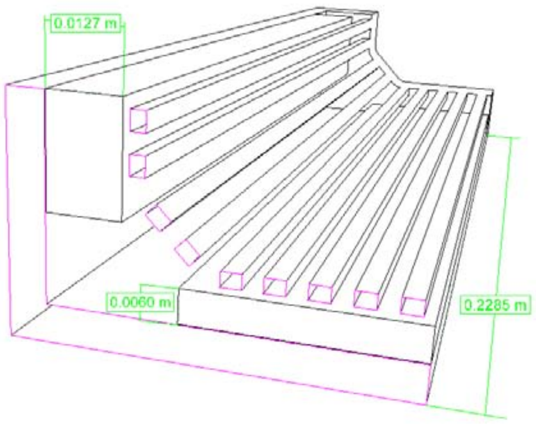

FIG. 18: IR absorber. One quarter.

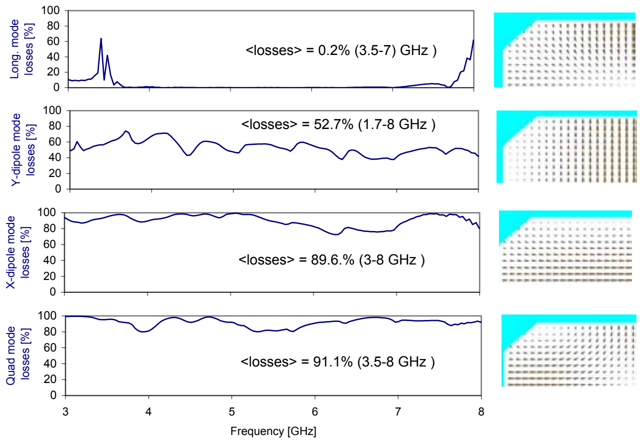

FIG. 19: Losses of different modes in IR absorber.

ence can be partially compensated by placing the thicker absorbing ceramic tiles at shorter sides. Figure 18 shows the geometry of IR absorber (one quarter). Horizontal size of the chamber is 88.4 mm and vertical size is 51 mm. The optimized value of the slot length is around 23 cm, the slot width is 3.4 mm. Absorber tile thickness is 6 mm at the long side and 12.7 mm at the short side. Absorption for longitudinal mode, two polarizations of the dipole mode and quadrupole mode are shown in Figure 19. In this device we managed to achieve almost 90% absorption of the dipole mode with horizontal polarization in the frequency range of 3-8 GHz and more than 50% absorption of the dipole mode with vertical polarization in the frequency range of 1.7-8 GHz. Absorption of the quadrupole mode is on average of 73% in the frequency range of 3.5-8 GHz. We keep the average absorption of the longitudinal mode at the level of 0.2% in the frequency range of 3.5 to 8 GHz. This absorber was mechanically designed and fabricated. It is already installed in the ring and we will soon measure HOM power in this absorber. Cooling system can take out up to 30 kW power.

V. CONCLUSION

We designed a new absorbing device for damping transverse wake fields. It is implemented in a straight section of PEP-II LER demonstrating the capability to remove and damp undesirable dipole and quadrupole propagating higher order modes produced at an upstream collimator with minimal impedance to the beam. As a result HOM contribution to beam line heating is reduced without impacting beam stability, allowing higher currents for increased luminosity.

Acknowledgments

We wish to acknowledge M.Kosovski, S.DeBarger, N.Kurita and N.Reeck for the mechanical design of the absorber and the PEP-II team for the help and fruitful discussions. Work supported by Department of Energy contract DE–AC02–76SF00515.

[1] J.Seeman et al, A Luminosity of $10^{34} cm^{-2} s^{-1}$ in the PEP-II B-factory, *in Proceedings of EPAC'2006, Edinburgh, Scotland*

[2] A.Novokhatski, S.DeBarger, F.-J.Decker, A.Kulikov, J.Langton, M.Petree, J.Seeman, M.Sullivan, "Damping the Higher Order Modes in the Pumping Chamber of the Pep-II Low Energy Ring", *in Proceedings of EPAC 2004*, Lucerne, Switzerland, p.854.

[3] A. Novokhatski, HOM effects in vacuum chamber with short bunches, *in Proceedings of 2005 Particle Accelerator Conference*, Knoxville, Tennessee, p. 289.

[4] T. Tajima, K. Akai, E. Ezura, T. Furuya, K. Hosoyama, S. Mitsunobu, The Superconducting Cavity Syste. for KEKB, *in Proceedings of 1999 Particle Accelerator Conference*, New York,p. 440.

[5] S.Blomestnykh et al, The Interaction between a Beam and a Superconducting Cavity Module: Measurement in CESR and CESR-Phase III Goals, Cornell SRF report 950905-12, 1995.

[6] H.Hahn, A.Burrill, R.Calaga, D.Kayran, Y.Zhao, R-square impedance of ERL ferrite HOM absorber, Physica C 441 (2006), p.239.

[7] Y.Suetsugu,T.Kageyama, Y.Takeuchi, K.Shibata, Development of wing-type HOM damper for KEKB, NIM in Phys. Res. A 533 (2004), p.295.

[8] S.Weathersby, M.Kosovski, N.Kurita , A.Novokhatski J.Seeman, A Proposal for a New HOM Absorber in a Straight Section of the PEP-II Low Energy Ring, *in Proceedings of 2005 Particle Accelerator Conference*, Knoxville, Tennessee, p.2173.

[9] S.Weathersby, M.Kosovski, N.Kurita, A.Novokhatski, J.Seeman, A New HOM Water Cooled Absorber for the PEP-II B-Factory Low Energy Ring, *in Proceedings of EPAC'2006, Edinburgh, Scotland*

[10] The MAFIA collaboration, User Guide CST GmbH, Darmstadt,

[11] S.Heifets, G.Lamberston, C.-K.Ng, Narrow-band Impedance of the PEP-II Collimators, SLAC-AP-122, April 1999.

[12] S.Kar, M.Leung, Experimental Studies on the PEP-II Low Energy Ring (LER) Collimator, CBP Technical Note #190, August 1999.

[13] R.Pendleton, K.Ko, C.Ng,M.Meubauer, R.Rimer, PEP-II B-factory Prototype Higher Order Mode Load Design, *in Proceedings of 1995 Particle Accelerator Conference*, Dallas, Texas, p.1800.

[14] Properties of Ceradyne's Advanced Technical Ceramics for Microwave Applications,Internet: www.ceradyne.com

[15] Montgomery, et all., "Principles of Microwave Circuits", M.I.T. Rad. Lab. Series, Vol.8 (1948).